Transport properties of artificial micro-swimmer and related nonequlibrium phenomenona

Summary of Work (5000 Words)

For the Award of Ph. D. (Sc.) Degree in Chemistry (Theoretical)

Submitted to

The Presidency University

by

Debajyoti Debnath

Registration No.: R-17RS205170094

Date of Registration: 10/7/2018

Presidency University

2020

Supervisor

Dr.Pulak Kumar Ghosh

CONTENTS

CONTENTS	Page No
Chapter 1-Introduction	**3-7**
Chapter 2	**8-13**
Chapter 3	**14-17**
Chapter 4	**18-19**
Chapter 5	**20-22**
Chapter 6	**23-24**
List of Publications	**25-26**

Chapter 1: Introduction

One of the emerging topics of current research in nanotechnology is to design nanometer -to - micrometer size motile particles whose movement can be controlled externally [1-3]. The most successful step to this direction is artificial active matter where particles are capable of moving by extracting kinetic energy from the surrounding medium [2,3]. Recently, a class of active particles have been synthesized where particles acquire self-propulsion taking advantage of local gradients produced by external energy sources [1-5]. Such particles consist of two distinct heme-spheres with completely different physical or chemical properties. The district heme-spheres may have different catalytic properties, photo-chemistry or exhibit different interactions with surrendering solvent molecules.

Figure 1.1: Schematic of Janus particles with distinct faces having different physical and chemical properties.

These types of two-faced particles known as Janus particles (named after the two faced Roman god Janus). Pierre-Gilles de Gennes mentioned the term "Janus" particle in his Nobel lecture in 1991. Although initially Janus particles were synthesized to prepare porous surfaces with appropriate surfactant, however it started receiving attention in chemical physics and biology when Sen et al [3] designed and synthesized a micro-sized Janus particle with one face containing platinum which can catalyze decomposition of hydrogen peroxide. These types of particles were synthesized to design 'nano-motors' for applications in biological sciences and nanotechnology. Thereafter, thinking of potential applications, several pioneer researchers have given significant input in this field of designing and characterizing self-propelled Janus particles with different goals. Few years later Sano et. [4]., synthesized a new type of self-propelled Janus particles which were powered by a different mechanism. Later on, Prof. Bechinger's group [5] (Universität Stuttgart, Germany) experimentally explore very interesting transport features self-propelled Janus particles in a patterned environment and have shown that such

active particle can be used as a light driven diffusing tracer. This pioneering work made self-propelled Janus particles more widely acceptable and versatile model systems for experimental tests of theories related to non-equilibrium phenomena [6-9]. The actual mechanisms of self-propulsion rest on some kind of phoretic process at the propeller - solvent interfaces. As for examples, suppose the self-propulsion is the result of chemical reactions or light absorption selectively one of the hemispheres. In the former case, asymmetric chemical gradients resulting from catalytic reactions push the particles to a specific reaction. Another example, selectively one hemisphere of the Janus particle becomes warmer by absorbing light. Thus, a fluid velocity gradient is produced at the vicinity Janus-particle solvent interface (see Fig.2.1).

Thanks to engines of their own, a class of Janus particles are capable of extracting kinetic energy from the surrounding medium. They are known as self-propelled Janus particles. Like living organisms, self-propelled Janus particles have the ability to move, in the absence of external drives.

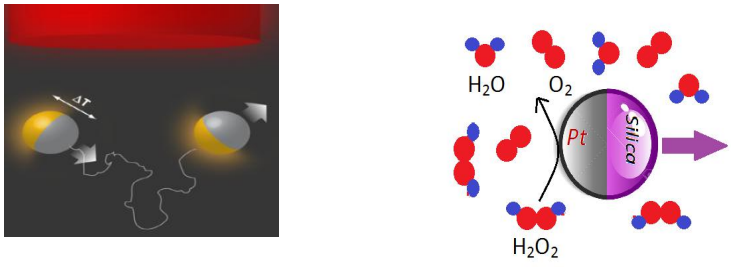

Figure 1.2: Schematic self-propulsion mechanisms. Left - Self-propulsion based on the thermo-phoresis. Right - diffusiophoresis is responsible for self-propulsion.

In most of the previous studies of the dynamics of Janus particles, generally, it was assumed that the velocity is directed along the self-phoretic force. The phoretic force acts with respect to specific particles' axes. Moreover, rotational diffusion as well as other non-equilibrium fluctuations keep the direction of self-phoretic change. As a result, Janus particles exhibit random motion, however, the net fluctuating forces acting on the particles are time correlated. Due to time corrected motion Janus particles can diffuse much faster than the passive Brownian particles of the same size (example, silica bead with radius 2.13 mm one hemisphere-coated

with 20 nm thick gold layer has diffusivity about 7.84 μm^2/second, where as a passive silica spheres have diffusivity about $0.03 \mu m^2$/second.

Janus particles exhibit very interesting and unusual transport features. When they diffuse through spatially periodic structures with broken inversion symmetry, interestingly, autonomous motion is observed. The spatial periodic structures can either be energetic potential or channel with varying cross-section. Note that in this interesting ratcheting effect detail balance is broken due to non-equilibrium correlated fluctuations of external origin. More interestingly, in some situations particles exhibit absolute negative mobility, that is, Janus particles spontaneously move to the opposite direction of the driving force.

Despite a considerable attention in understanding dynamics of self-propelled micro- and nanoparticles, still some fundamentally important issues remain unexplored. They are listed below:

(1) In most of the experiential situations due to fabrication defects system of micro-swimmer comprise of particles with various self-propelled velocities. Even in the natural micro-swimmer (e.g. Sperm Cells) one finds a large variation of self-propulsion among swimmers. To gain control over dynamics of the particles in such a mixture it is essential to have an idea about how the dynamics of fast moving particles is affected by the slower moving one or vice-versa. We can pose the same question in another way: How to improve velocity, diffusivity or effusivity of slower moving particles by adding fast moving particles ?

(2) Most of the previous studies focus on the diffusion of micro-swimmer in the absence of flow field. However, in many physical situations, active or passive particles diffuse under the influence of some flow field due to density fluctuation or other types of effects. Therefore, it is desirable to know effect of flow field on the diffusion of self-propelled particles.

(3) As the active particles exhibit time correlated Brownian motions, in the many cases they exhibit a long diffusion transient which could be potentially important in fluctuation-induced non-equilibrium phenomena. Such type situations, where transient effects are important, the actual diffusion mechanism is largely unknown.

(4) The nano-technological application involves diffusion of particles through various types of confined structures where inertia effect may play dictating roles. However, interplay between self-propulsion and inertia in the confined structures are largely unknown.

The present thesis addressed the above mentioned issues based on the simulation of dynamics of Janus particles. The thesis is organized as follows. In Chapter I, we present the introduction of self-propelled Janus particles and briefly describe significance of our works in the context of previous works in this field as well as applications in nanotechnology and medical sciences. Chapter 2 presents transport properties of Janus particles in a binary mixture of two kinds of swimmers in the under-damped limit. Based on the numerical simulation we show the presence of strong Janus particles considerably improves velocity distribution of weak particles. In the Chapter 3, we show that even in the absence of inertia, motility can transfer from weak to strong particles in the binary mixture. This has been confirmed by studying how effusion of weak particles changes by the presence of passive particles.

Chapter 4 presents diffusion of self-propelled Janus particles in the counter rotating convection rolls. We focus on the large Péclet numbers, i.e., for self-propulsion speeds below a certain depinning threshold and weak rototranslational fluctuations. In this limit the particle undergoes asymptotic normal diffusion with diffusion constant proportional to the square root of its diffusion constant in the absence of flow. We model Chirality effects in the propulsion mechanism assuming a tunable applied torque which induce particle jumping between adjacent convection rolls. The jumping mechanism among adjacent convection rolls can be identified by an excess diffusion peak.

In the Chapter 5, we explore interplay between inertial relaxation to the time correlated self-propelled motion in confined structures. This issue is potentially important as most of the novel nano-technological applications of Janus particles involve diffusion through different types of confined structures where inertial impact as well as self-propulsion. We address this issue and show that inertial impact is important in the experimentally accessible situations for both self-propelled and passive particles. In Chapter 6 we present a summary of our works and possible future directions.

References

[1] F. Schweitzer, Brownian Agents and Active Particles (Springer, Berlin, 2003); P. Romanczuk et al, Eur. Phys. J. Special Topics 202, 1 (2012).

[2] S. Ramaswamy, Annu. Rev. Condens. Matter Phys. **1**, 323 (2010).

[3] W. F. Paxton, S. Sundararajan, T. E. Mallouk, and A. Sen, Angew. Chem., Int. Ed. 45, 5420 (2006); J. G. Gibbs and Y.-P. Zhao, Appl. Phys. Lett. 94, 163104 (2009); J. R. Howse, R. A. L. Jones, A. J. Ryan, T. Gough, R. Vafabakhsh, and R. Golestanian, Phys. Rev. Lett. **99**, 048102 (2007).

[4] H. R. Jiang, N. Yoshinaga, and M. Sano, Phys. Rev. Lett. 105, 268302 (2010).

[5] G. Volpe, I. Buttinoni, D. Vogt, H.-J. Ku¨mmerer, and C. Bechinger, Soft Matter 7, 8810 (2011).

[6] P. K. Ghosh, V. R. Misko, F. Marchesoni, and F. Nori, Phys. Rev. Lett. 110, 268301 (2013).

[7] P. K. Ghosh, P. Hänggi, F. Marchesoni, and F. Nori, Phys. Rev. E 89, 062115 (2014).

[8] P. K. Ghosh, F. Marchesoni, S. Savel'ev, and F. Nori, Phys. Rev. Lett. 104, 020601 (2010).

[9] Non-Gaussian Normal Diffusion in a Fluctuating Corrugated Channel Li, F. Marchesoni, D Debnath, P. K. Ghosh, Physical Review Research 1, 033003(2019).

[9] Diffusion of chiral janus particles in convection rolls, Y Li, L Li, F Marchesoni, D Debnath, PK Ghosh, Physical Review Research 2 (1), 013250 (2020).

[10] Diffusion of chiral janus particles in convection rolls, Y Li, L Li, F Marchesoni, D Debnath, PK Ghosh, Physical Review Research 2 (1), 013250 (2020).

[11] Enhanced motility in a binary mixture of active nano/microswimmers, D. Debnath, P. K Ghosh, V. R Misko, Y. Li, F Marchesoni, F Nori, Nanoscale 12 (17), 9717-9726 90 (2020)

[12] Non-Gaussian Normal Diffusion in a Fluctuating Corrugated Channel Li, F. Marchesoni, D Debnath, P. K. Ghosh, Physical Review Research 1, 033003(2019).

Chapter 2

Motility transfer from strong self-propeller to weak ones to improve kinetic energy and velocity distribution

Introduction

In nanotechnology, material and biological sciences it is often desirable to enhance the diffusivity and effusivity of active nano- or microscale swimmers. Examples include, self-propelled Janus particles as agents for accelerating chemical transformations or to energize slowly moving sperm cells for better chances of successful fertilization. Here we tackle this problem based on the idea that motility can be transferred from a more active guest species to a less active host species. We performed numerical simulations of motility transfer in two typical cases, namely for interacting particles with weak inertia effect, by analyzing their velocity distributions, and for interacting overdamped particles, by studying their effusion rate. In both cases we detected motility transfer with a motility enhancement of the host species of up to a factor of four. This technique of motility enhancement can find applications in chemistry, biology and medicine.

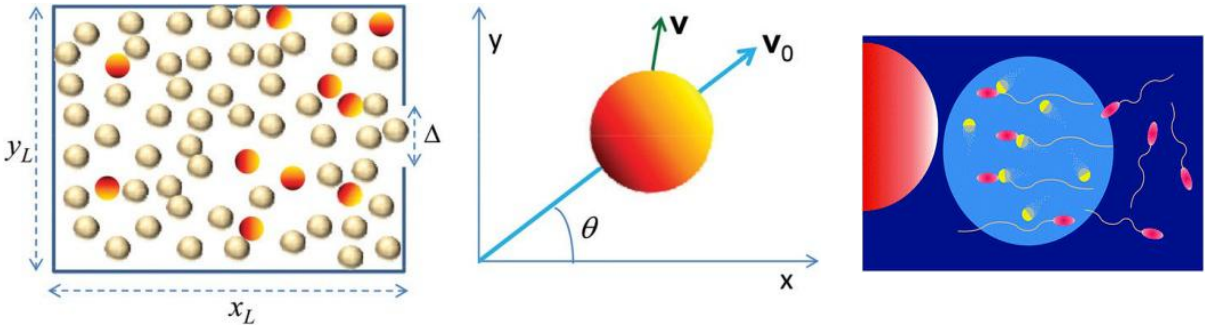

Figure 2.1: Left: Schematic of a mixture of self-propelled particles in a rectangular box $x_L \times y_L$ with an opening of width Δ. Middle: Schematic of a two-dimensional self-propelled Janus Particle. Its dynamical, v, and self-propulsion velocities, v_0, are depicted by distinct vectors. Right: Schematic of motility transfer between weak and strong propellers.

Model: To explore the above mentioned issues, consider a system consisting of two types of Janus Particles with different self-propulsion speeds in a thermal bath. For very short distances they interact with each other via a truncated Lennard-Jones potential,

$$\left.\begin{aligned} V_{ij} &= 4\varepsilon\left[\left(\frac{\sigma}{r_{ij}}\right)^{12}-\left(\frac{\sigma}{r_{ij}}\right)^{6}\right], \qquad r_{ij}\le r_m \\ &= 0 \qquad \text{otherwise} \end{aligned}\right\} \text{- - - - (2.1)}$$

Where ε is the interaction constant, r_m locates the potential minimum, and $\sigma = 2r_0$. For sake of simplicity we ignored hydrodynamic interactions. Here we calculate the particle's velocity distributions to establish the relationship of the motility of the two species.

The dynamics of the particles in the xy-plane can be described by the following set of Langevin equations

$$m\ddot{\mathbf{r}}_i = -\gamma\dot{\mathbf{r}}_i + +\sum_j \mathbf{F_{ij}} + \gamma\mathbf{v_0} + \boldsymbol{\xi}_i(t) \quad . \; . \; . \; (2.2)$$

$r_i \equiv (x_{i,}\, y_i)$ denoted the instantaneous position of the i-th particle and $\xi(t)$ are the thermal fluctuations which are modeled by Gaussian white noises. $\mathbf{F}_{ij}$ and $\mathbf{v}_0$, inter particle forces and self-propulsion, respectively. The direction of self-propulsion changes in a random manner due to rotational diffusion. We characterized the rotational diffusion (D_θ) by the time constant τ. The thermal diffusion of the particle is, $D_0 = kT/\gamma$. Here γ plays the role of an effective damping constant. We numerically integrated Eqs. (2.2) to obtain the velocity distributions and effusion rates.

Results and Discussion: It is well known that the velocity of overdamped Brownian particles is an ill-defined quantity. Indeed, mass less particles undergo a displacement only during the action of external forces , here thermal fluctuations, collisions against other particles or the box walls, and the effective self-propulsion forces. Therefore, to extract a velocity distribution, one needs to simulate inertial effects. By numerically integrating the coupled eqn (2.2)–(2.4), we systematically analyzed velocity distributions in systems of non-interacting and interacting active JPs, as well as in binary mixtures of two species of JPs with different self-propulsion speeds

Velocity distribution of non-interacting Janus particles: We first consider the case of a single species of non-interacting particles self-propelling in a thermal bath of temperature T with speed v_0. Velocity distribution at different values of the rotational diffusion constant, D_θ , are shown in Fig. 2.2(a). The inertial effects become important as the viscous relaxation time constant, $\tau_\gamma = 1/\gamma$, grows comparable or greater than the rotational relaxation time $\tau_\theta = 1/D_\theta$. When $\tau_\gamma >> \tau_\theta$ (or $\gamma << D_\theta$), the velocity distributions are mostly determined by thermal fluctuations and in the opposite regime, $\tau_\gamma << \tau_\theta$ (or $\gamma >> D_\theta$), self-propulsion effects play the main role. Figure 2.2(a) shows the transition from self-propulsion to inertia-dominated regime.

At asymptotically large observation times, a free Janus Particle behaves like a persistent Brownian particle with effective temperature

$$T_{eff} = \frac{\gamma}{k}\left(D_0 + \frac{v_0^2}{2D_\theta}\right)^2 \text{- - - - (2.3)}$$

and persistence length $l_0 = v_0\tau_0$. For large values of D_θ, particles velocities must be distributed as-

$$p(v) = \left(\frac{mv}{kT}\right)\exp\left(-\frac{mv^2}{2kT}\right) \text{- - - - (2.4)}$$

Fig.2.2(a) supports this fact. When the self propulsion length of the active particle is set much larger than its thermal length and temperature is lower than velocities must be distributed as

$$p(v) = \left(\frac{1}{\sqrt{2\pi\gamma D_0}}\right)\exp\left[-\frac{(v-v_0)^2}{2\gamma D_0}\right] \text{- - - - (2.5)}$$

Velocity distribution of interacting Janus particles: Velocity distributions for different values of the packing fraction, $\phi = 4r_0^2 N_t/(x_L + 2r_0)(y_L + 2r_0)$ are displayed in Fig. 2.2(b). With $\phi > 0.5$, interacting active Janus Particles obey the Maxwellian velocity distribution,

$$p(v) = \frac{v}{B}\exp\left[-\frac{v^2}{2B}\right] \text{- - - - (2.6)}$$

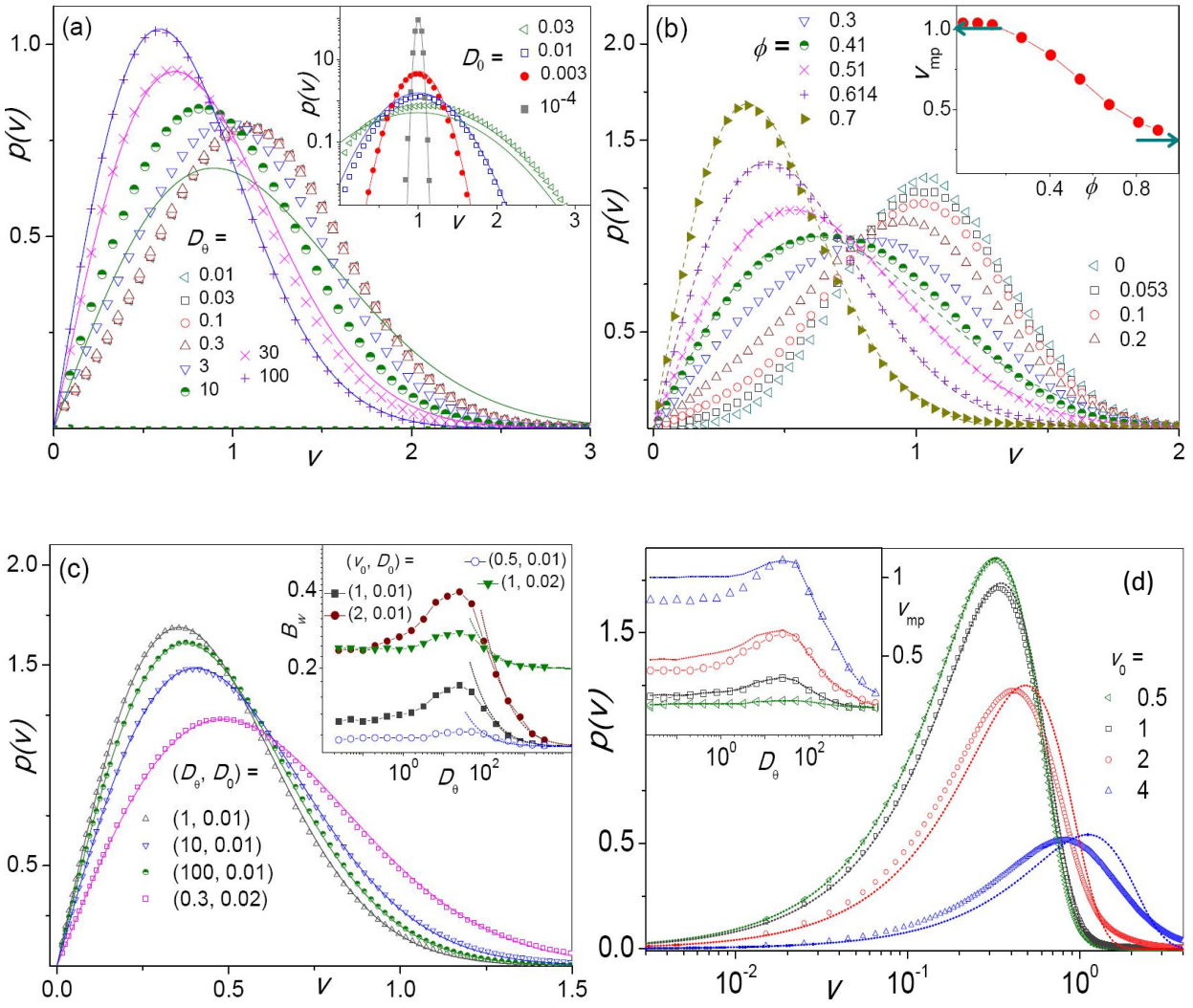

Figure 2.2: (a) Velocity distribution of non-interacting active Janus Particles for different D_θ. The inset illustrates the effect of thermal noise for D_θ = 0.3. Symbols denote numerical simulation data; solid lines are the analytical estimates of Eq. (2.4), main panel, and Eq. (2.5), inset. The parameters used are (unless reported otherwise in the legends): D_θ = 0:03; v_0 = 1; γ = 10; m = 1. (b) Velocity distribution of interacting self-propelled particles for different the packing fraction. Velocity distribution of interacting self-propelled particles for different rotational diffusion. (c) Velocity distribution of interacting self-propelled particles for different D_θ. (d) Velocity distribution of interacting self-propelled particles for different self-propulsion strength.

B, depends on the T, D_θ, v_0, and ϕ. We investigate the effect of self-propulsion on the velocity distribution in a dense system, and plot the result in Fig.2.2(c). In the inset, we plotted width of p(v) against D_θ.

For very slow rotational relaxation, the width of the distribution is almost independent of D_θ. In this regime, the self-propulsion length l_θ is much larger than the average effective inter-particle distance l_s, so that the particle free path cannot exceed l_s. The fitting parameter seems to obey the empirical law, $B = \gamma(D_0 + \alpha v^2)$, with α a function of the packing fraction. This result can be explained by comparing B with kT_{eff} in eqn (2.3). In the opposite limit, $l_\theta < l_s$, the active particles manage to change their direction before colliding with other particles, so that their inter-

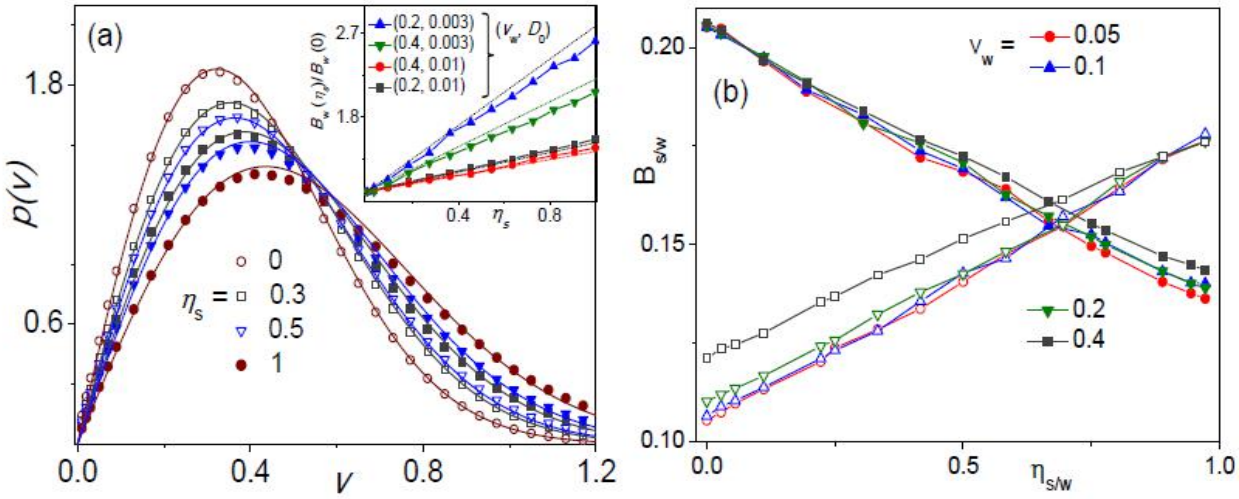

Figure 2.3: Comparison of velocity distribution p(v) of weak (empty symbols) and strong (filled symbols) active particles with varying composition η_s of the binary mixture. Note that solid (hollow) circles represent velocity distribution of strong (weak) active particles for the interacting single species case. Solid lines correspond to eqn (8) where B is obtained from least-squares fittings. Inset plots depict the variation of distribution width of weak JPs B_w as a function of the fraction of strong active particles, $\eta_s = N_s/N_t$. Thus, $\eta s = 0$ means that all particles are weak and $\eta_s = 1$ that all particles are strong. Dotted lines represent eqn (9) with the relevant best-fit parameters α_s and α_w. (b) Distribution widths of weak, B_w (empty symbols), and strong active JPs, B_s (filled symbols), respectively versus η_s and η_w for different

collisional dynamics is dominated by the elf-propulsion dynamics. They behave as if they were floating in a thermal bath with the effective temperature of eqn (2.3). The ensuing estimates of

the distribution fitting parameter, $B = \gamma(D_0 + v^2\tau_\theta/2)$, drawn in the inset of Fig. 2.2(c) fairly agree with the numerical data.

Velocity distribution in binary mixture: Let us consider now a mixture of active particles of two types. Let us denote the N_w particles with fixed self-propulsion speed v_w, as weakly active, and the remaining Ns particles with tunable self-propulsion velocity vs, as strongly active. A comparison of velocity distributions of the weak (hollow symbols) and strong (solid symbols) JPs in a binary mixture is shown in Fig. 2.3(a) for different fractions $\eta_s = N_s/N$ of the strong active particles. Plots here correspond to situations where the system packing fraction ϕ is quite large and the velocity distributions p(v) are of the Maxwellian type, eqn (2.8). As to be expected, the plots in Fig. 2.3(a) show that weak active particle distributions grow wider, and their maxima shift to higher velocities, with increasing ηs. On the other hand, the distributions of the stronger component shrink and their maxima shift toward lower velocity values in comparison with the single component system. This result suggests an effective motility transfer from more active to less active particles.

References:

[1] Janus Particle Synthesis, Self-Assembly and Applications, ed. S. Jiang and S. Granick, RSC, Cambridge, 2012.

[2] S. Krishnamurthy, S. Ghosh, D. Chatterji, R. Ganapathy and A. K. Sood, A micrometre-sized heat engine operating between bacterial reservoirs, Nat. Phys., 2016, 12, 1134

[3] J. R. Howse, R. A. L. Jones, A. J. Ryan, T. Gough, R. Vafabakhsh and R. Golestanian, Self-Motile Colloidal Particles: From Directed Propulsion to Random Walk, Phys. Rev. Lett., 2007, 99, 048102.

[4] Enhanced motility in a binary mixture of active nano/microswimmers, D. Debnath, P. K Ghosh, V. R Misko, Y. Li, F Marchesoni, F Nori, Nanoscale 12 (17), 9717-9726

Chapter 3

Enhanced effusivity in the binary mixture of overdamped self-propelled particles

Introduction

In the previous chapter, we showed how adding a relatively small fraction of highly motile microswimmers to a suspension of less motile microswimmers can considerably enhance the overall motility of the mixture. This effect was demonstrated in the presence of inertia. We consider now the limiting case of overdamped, or massless, active particles. This limit corresponds to low Reynolds numbers, a hydrodynamic regime that applies to most microswimmers investigated in the literature, both biological and artificial. This raises a problem, because, as mentioned above, the velocity distribution of massless particles is mathematically ill-defined. To avoid this difficulty, in our simulations we computed an alternative motility quantifier for the overdamped limit, namely the effusion rate of the active JPs through a narrow pore of the simulation box. The corresponding Langevin equations in the highly damped situation are obtained by ignoring inertia,

$$\dot{\mathbf{r}}_i = \sum_j \mathbf{F_{ij}} + \mathbf{v_0} + \boldsymbol{\xi}_i(t) \quad . \; . \; . \; (3.1)$$

Based on the numerical simulation of the above equation, the effusion rate has been studied in depth to characterize classical transport in constrained geometries. We define the effusion rate of the strong (s) [weak (w)] JPs, Es (E_w), as the number of s (w) particles exiting the simulation box per unit time.

Effusion of non-interacting particles: In the case of a single-component system, we denote the effusion rate by E_m. Let us consider the effusion rate $E_m(0)$ of a single species of non-interacting JPs. In Fig. 3.1(a) we plotted a few curves $E_m(0)$ versus v_0 for different values of D_θ. For $v_0 \rightarrow 0$, the effusion is controlled by thermal motion and, as expected, is insensitive to v_0. Effects due to self-propulsion become appreciable only for values of v_0 larger than the particle thermal speed. Beyond certain threshold value, the effusion rate grows first quadratically with v_0 and then saturates toward an asymptotic value. The rising branches occur for $l_\theta << x_L, y_L$. Indeed, for very

short rotational relaxation times, when it can safely be assumed that particles diffuse in a thermal bath with effective constant , the effusion rate through a narrow pore reads as follows [1,2].

$$E_i(0) \approx x_L y_L \rho_i D_\theta / \pi$$

Effusion of interacting particles

The effusion rate of interacting self-propelling particles with $\varepsilon > 0$ is plotted in the inset of Fig. 3.1(a). This figure shows the v_0-dependence of the effusion rate relative to the corresponding rate in the absence of interaction, $E_m(\varepsilon)/E_m(0)$, for several values of D_θ. The system we simulated here was quite dense ($\phi = 0.66$), so that the self-propulsion mechanism agreement with the data plotted in the inset of Fig. 3.1(b). In the very strong self-propulsion regime, both $E_m(\varepsilon)$ and $E_m(0)$ tend to saturate [see Fig. 3.1(b)]. However, $E_m(\varepsilon)$ saturates at larger v_0 values than in the non-interacting case. A plausible explanation is suggested by a comparison of the mixture snapshots. The particles far away from the walls are more mobile and contribute more to the effusion rate; they are not jammed against the walls and "see" a larger opening-width to compartment size ratio, Δ/y_L. In contrast, particles jammed against the walls tend to clog the box opening. However, the fraction of the more mobile particles drops fast with increasing v_0, thus leading to plateaus in the effusion rate in the limit $v_0 \to \infty$.

Figure 3.1(c) illustrates the dependence of the effusion rates of the two active mixture components on their self-propulsion parameters, v_0 and D_θ. The mixture is of 1 : 1 molar ratio of strongly (s) and weakly (w) active particles. We kept the self-propulsion speed v_w fixed and varied vs from values lower to values higher than v_w. First of all, we notice that the effusion rates of both JP species are almost insensitive to the rotational diffusion for $v_s \to 0$, while developing a strong dependence on D_θ in the opposite limit, $v_s \to \infty$. For $v_s > 10v_w$, at $D_\theta = 1$ the effusion rate is about one order of magnitude larger than that at $D_\theta = 0.1$.

In conclusion, we stress that adding a small amount of strongly active JPs does suffice to enhance the effusion of sluggish active JPs, but an excess of them can produce the opposite effect! Recall that, as illustrated by our simulation snapshots, the two components of an active binary mixture can separate into two distinct phases, when the self-propulsion length of one component is much larger than the size of the container and the other one much shorter, that is, for $v_s/D_\theta >> x_L, y_L >> v_w/D_\theta$. However, phase segregation should be avoided for better motility transfer.

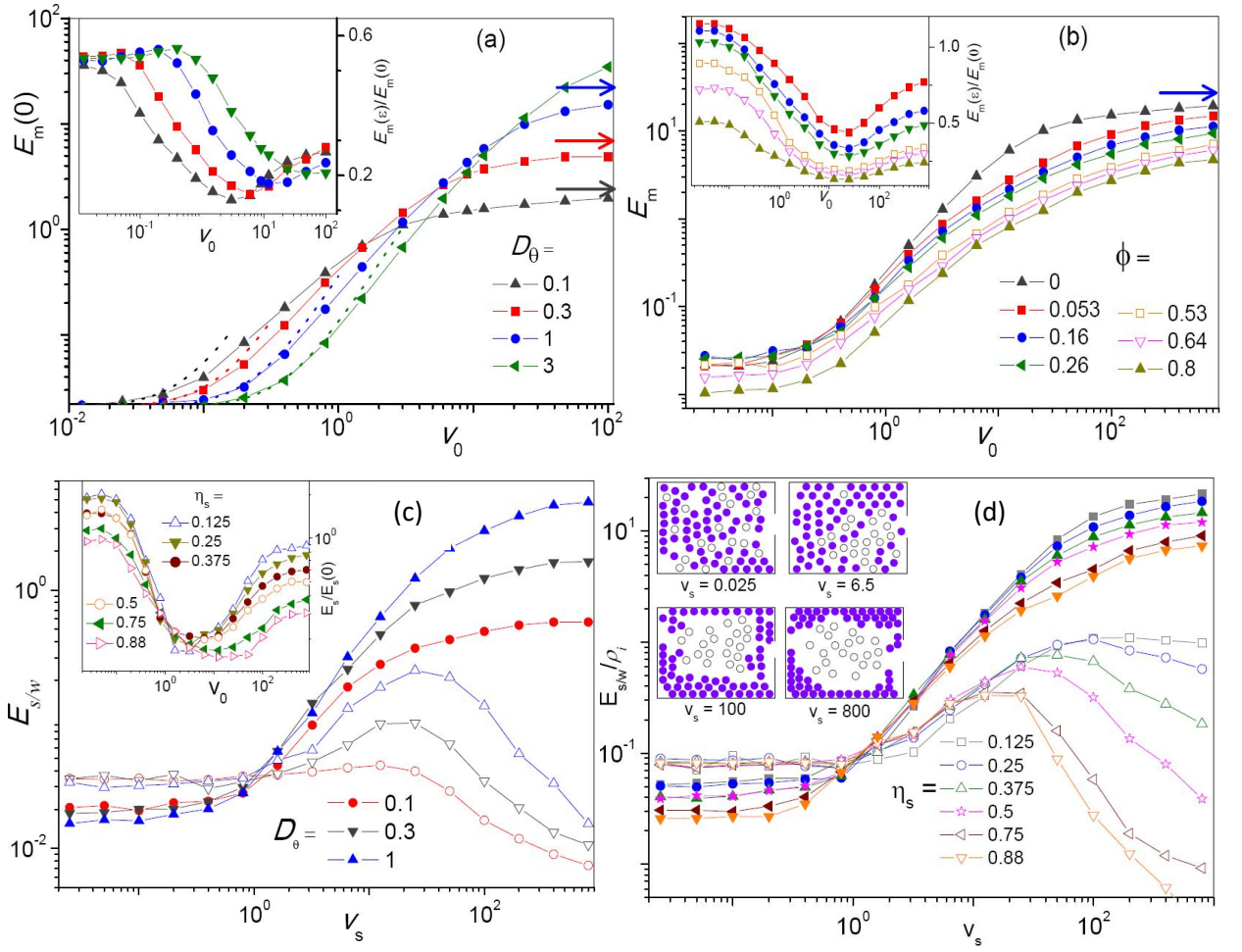

Figure 3.1: (a) Effusion rate of non-interacting JPs as a function of the self-propulsion velocity for different rotational diffusion coefficient. (b) Effusion rate of interacting self-propelled particles versus v_0 for $\varepsilon = 1$ and different packing fraction ϕ. (c) Effusion rates E_s (filled dots) and E_w (empty dots) versus vs for binary mixture with $\eta_s = 0.5$ and different values of D_θ (see legends). Inset: Effusion ratio of stronger component, $E_m(\varepsilon)/E_m(0)$ versus v_0 for different ηs and $D_\theta = 1$. (d) Effusion rates E_s (filled dots) and E_w (empty dots) versus vs in a binary mixture for $D_\theta = 1$ and different η_s (see legends). Inset: Snapshot of binary mixture with $\eta_s = 0.75$, $D_\theta = 1$ and different v_s [0.025 (top-left), 6.5 (top-right), 100 (bottom-left), and 800 (bottom-right)].

References:

[1] D. Holcman and Z. Schuss, Stochastic Narrow Escape in Molecular and Cellular Biology, Springer, New York, 2015.

[2] P. K. Ghosh, Communication: Escape kinetics of self-pro pelled Janus particles from a cavity: Numerical simulations, J. Chem. Phys., 141, 061102 (2014,)

[3] Enhanced motility in a binary mixture of active nano/microswimmers, D. Debnath, P. K Ghosh, V. R Misko, Y. Li, F Marchesoni, F Nori, Nanoscale 12 (17), 9717-9726 (2020)

Chapter 4

Diffusion of self-propelled Janus particles in the presence of fluid flow field

Recently, artificial microswimmers found promising applications in the pharmaceutical (e.g., smart drug delivery [1]) and medical research (e.g., robotic microsurgery [2]), whereby one expects that the function they are designed to perform is governed in time and space by their diffusive properties. To this regard it is important to control the diffusion of active particles in crowded and patterned environments, where they interact with other system components, either chemically or mechanically. Even more important for applications to cell biology and chemical industry, requires regulating their diffusion in hydrodynamically active mediums[2].

To this purpose, we investigated the diffusion of a single overdamped JP with self-propulsion speed v_0 suspended in a length of the flow unit cell. As illustrated in Fig.4.1, ψ(x, y) defines four counter-rotating advection subcells.

$$\psi(x,y) = (U_0 L/2\pi)\sin(2\pi x/L)\sin(2\pi y/L) \quad \text{- - - -(4.1)}$$

Particle transport in such a flow pattern has been studied under diverse conditions. For instance, in the presence of periodic perturbations the deterministic dynamics of a passive particle exhibits remarkable chaotic properties. However, despite its practical implications, the problem of how a flow field with stream function like ψ(x, y) can affect the diffusion of self-propelled particles has not been fully investigated, yet.

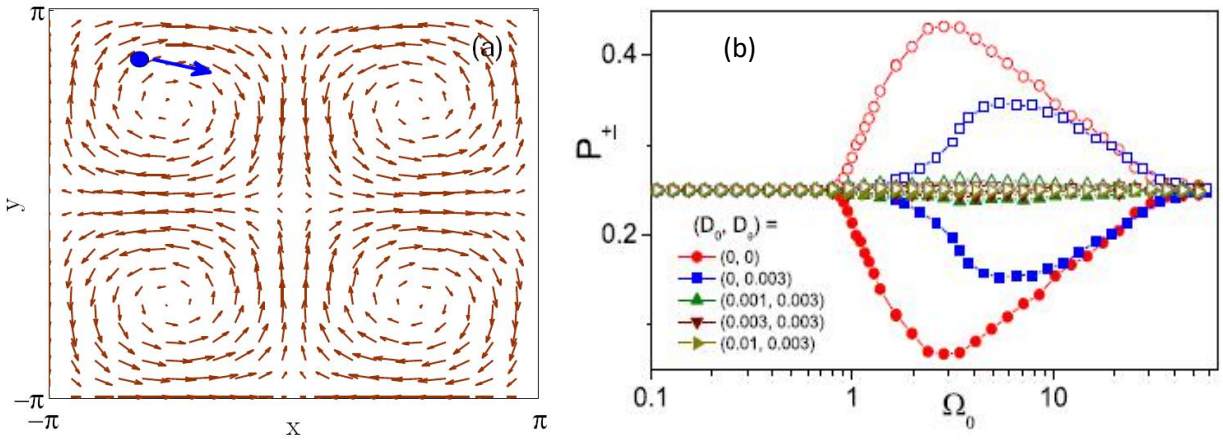

Figure 4.1: (a) Unit flow cell with steam function of Eq. (4.1), consisting of four counter-rotating subcells. (b) Particle probability density integrated respectively over a positive (P_+, solid symbols)

and a negative subcell (P_-, empty symbols), vs external torque Ω_0 for different values of the rotational and translational diffusion D_θ

We consider the more realistic situation of an active particle subject to both translational and orientational fluctuations. As a consequence, the direction of its self-propulsion velocity is driven not only by the local flow shear and, possibly, a chiral (applied or intrinsic) torque, but also by an intrinsic rotational noise. Moreover, due to thermal fluctuations, random hopping between convection rolls can occur even for self-propulsion speeds below the trapping threshold. We have shown that active diffusion in the laminar flow of Eq. (1) develops two distinct regimes, respectively for low and high chirality, both with a peculiar dependence on the particle self-propulsion parameters. At the transition, the chiral and shear torque compensate each other inside two diagonally opposite $\psi(x, y)$ subcells; this causes a partial depinning of the active particle from the convection rolls with a consequent diffusivity surge.

References:

[1] Janus Particle Synthesis, Self-Assembly and Applications, edited by S. Jiang and S. Granick (RSC, Cambridge,2012).

[2] M. C. Marchetti, J. F. Joanny, S. Ramaswamy, T. B. Liverpool, J. Prost, M. Rao, and R. A. Simha, Hydrodynamics of soft active matter, Rev. Mod. Phys. **85**, 1143 (2013).

[3] Diffusion of chiral janus particles in convection rolls, Y Li, L Li, F Marchesoni, D Debnath, PK Ghosh, Physical Review Research 2 (1), 013250 (2020).

Chapter 5

Transport of self-propelled particles through narrow channels

It is often desirable to know the controlling mechanism of survival probability of nano - or microscale particles in small cavities such as, e.g., confined submicron particles in fiber beds of high-efficiency filter media or ions/small molecules in confined cellular structures. Here we address this issue based on numerical study of the escape kinetics of inertial Brownian colloidal particles from various types of cavities with single and multiple pores. We consider both the situations of strong and weak viscous damping. Our simulation results show that as long as the thermal length is larger than the cavity size the mean exit time remains insensitive to the medium viscous damping. On further increasing damping strength, a linear relation between escape rate and damping strength emerges gradually. Further, we show that the effects of pore structure variation on the escape kinetics are conspicuously different in the low damping regimes compared to the overdamped situation. Apart from direct applications in biology and nanotechnology, our simulation results can potentially be used to understand diffusion of living or artificial micro/nano objects, like, bacteria, virus, Janus Particle etc. where memory effects play dictating roles.

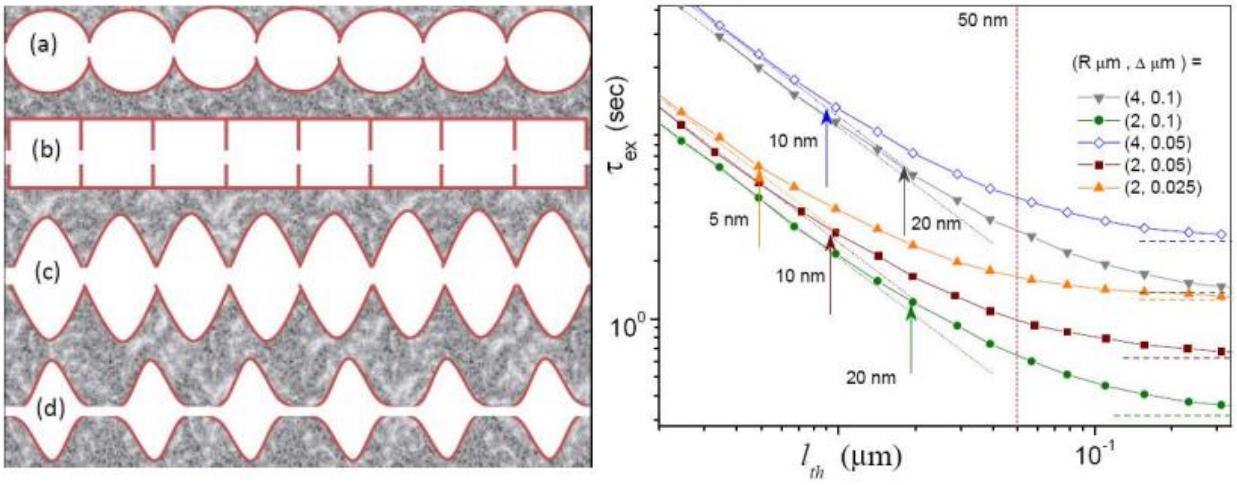

Figure 5.1: Left: Schematics of periodic channel formed by connecting various types of cavities [(a) circular, (b) rectangular, (c) and (d) corrugated channel compartments with different pore structures] . Right: . Thermal length versus exit time from a circular cavity. The vertical arrows depict the lower bounds of thermal length below which inertial effect can safely be ignored. The

numerical values of the lower bounds given next to the arrows. Vertical dashed line at lth = 50 nm indicates appropriate upper bound of thermal length of micron size particles under physically feasible conditions.

In overdamped limits, it is known that the mean exit time is inversely proportional to the thermal length l_{th} irrespective of the pore geometries. The deviation from this inverse relation is attributed to the inertial impact in the escape kinetics. Our simulation results [see Figure 5.1] show that inertial impacts become noticeable for the thermal lengths as small as 5 nm, 10 nm and 20 nm when pore widths are respectively 25 nm, 50 nm and 100 nm larger than the particle's diameter. Thus, impacts of underdamped motion in the escape kinetics can be accessed in experiments if the particle's thermal length is 5 nm or larger. The point up to which underdamping is meaningful (indicated by vertical arrows in the following Figure 5.1) depends on the exit window size and insensitive to the cavity size.

For a particle of size 1 micron and mass density 2g/cm^3 , l_{th} is about 0.6 nm (water) and 30 nm (air). Again it can be tuned to some extent by changing particle size, mass density and temperature.

$$l_{th} = \frac{m}{6\pi\eta_{\text{v}}\, r_0}\sqrt{\frac{k_B T}{m}} \;\propto\; \frac{\sqrt{r_0\,\rho T}}{\eta_{\text{v}}}$$

Thus, the thermal length of micron size particles at room temperature can fall in the range 0.1 nm to 50 nm depending upon the medium viscosity and mass density of the colloids. This estimate shows that inertial effects can easily be accessed in the experiments.

Note that our observable is the escape time from a cavity which involves diffusion over a length much larger than the particle size. Our simulations assume cavities of radius 2 to 5 times of particle's size. More importantly, as mentioned earlier, the thermal length up to which inertial effect cannot be discarded is insensitive to the cavity size. Inside the cavity, the particle's ballistic motion persists up to the thermal length l_{th} which is in practice much smaller than both the cavity and particle sizes. However, it can be comparable to the effective pore size (cavity bottleneck diameter minus particle diameter) in physically feasible conditions. Our simulation results in the above figure show that inertial impact persists in the escape kinetics until the particle's thermal length is as small as 20 % of the effective pore size. This is due to the fact that the short-range ballistic motion, being relevant around exit windows, changes the course of the

dynamics inside the cavity. Thus, conspicuously, short lived ballistic motions leave a noticeable impact on the escape kinetics. For experimental demonstration of inertial impacts thermal length need not be larger than the particle size.

References:

[1] D. Holcman and Z. Schuss, Stochastic Narrow Escape in Molecular and Cellular Biology, Springer, New York, 2015.

[2] P. K. Ghosh, Communication: Escape kinetics of self-propelled Janus particles from a cavity: Numerical simulations, J. Chem. Phys., 141, 061102 (2014)

[3] S. Nayak, T. Debnath, S. Das, D. Debnath, P. K Ghosh, J. Phys Chem C, 124, 34, 18747–1875 (2020).

Chapter 6

Summary and Further Extensions

Summary: Self-propelling Janus particles (JPs), the most common class of artificial microswimmer, have been the focus of widespread attention over the last two decades due to their emerging applications in nano-technology and medical sciences. Such particles are made by coating one hemisphere with catalytic or photo-sensitive or magnetic materials. Under appropriate conditions, one hemisphere undergoes physical or chemical changes with respect to the other, thus producing some local gradient in the suspension fluid (self-phoresis). This strategy allows artificial swimmers to propel themselves by harvesting energy from their environment.

Thanks to their self-propulsion mechanism and in contrast to their passive peer, artificial swimmers can diffuse orders of magnitude faster are capable of performing autonomous motion in periodic structures with broken spatial symmetry and exhibit other peculiar transport properties.Inspired by these unique transport features, researchers aim to design customized JPs to be used, for instance, as ``nano-robots'' capable of performing accurate mechanical operations.

For novel and emerging applications it is desirable to have control over the motion of the self-propelled particles when they are monitoring motion of a crow of passive particles or other self-propellers, or diffusing in the flowing fluids or passing through narrow channels. This thesis is particularly focused to address these issues.

We have shown that motion of weak propellers or passive particles can be monitored by adding strong propellers. It works through effective motility transfer from strong propellers to weak ones. Motility transfer mechanism has been established through careful inspection velocity distribution and effusivity in the binary mixtures.

In most practical situations, the diffusion process is not free from flow fields. Therefore, before embarking upon specific nano-technological applications, it is essential to know diffusivity in the presence of flow fields. We simulate dynamics of a Janus particle in the four counter rotating convection rolls and systematically investigate very rich phenomenology there.

Future extensions: Our simulation results in binary mixture suggested that motility transfer in the overdamped regime associated with non-trivial dynamics of weak and strong JPs. We recognized some parameters of the regime of self-propulsion, where a totally different effusion rate through motility transfer is observed. Large variation of effusion associated to change in spatial distribution of phase points, some of which show very crowded and uncooperative motions, while others seem to act as one resulting in better cooperativity. Now the key issue we want to explore is the degree of cooperativity and its functional dependence on self-propulsion properties of both types of species in binary mixture. In general, cooperativity is quantified by estimating the following quantity.

$$N_X^{Co}(t) = 1 + \frac{\sum_{i \neq j} \langle X_i X_j \rangle}{\sum_i \langle X_i \rangle}$$

Where, $X_i(t) = r_i(t)-r_i(0)$, is the displacement of the i-th particle over time t. For uncorrelated motion, the above quantifier is one. Positive or negative value associated with some type of correlated motion. To understand in more detail the effects of correlated movement, in addition to the above quantifiers we also want to calculate pair distance and cooperativity of nearest neighbor particles.

Other issues, accessing impact of interplay between flow field and confinement in the transport properties of artificial swimmers like Janus particles, would be an important and essential extension of the present study.

Publications

1. Communication: Cargo towing by artificial swimmers, **D Debnath**, P. K Ghosh**,** Y Li, F Marchesoni, B Li, Journal of Chemical Physics 145 (19), 191103 (2016).
2. Diffusion of eccentric microswimmers, **D Debnath**, P. K Ghosh**,** Y Li, F Marchesoni, B Li, Soft matter 12, 2017-2024 (2016).
3. Nonlocality of relaxation rates in disordered landscapes, Y Li, **D Debnath**, P. K Ghosh, F Marchesoni, The Journal of Chemical Physics 146 (8), 084104 (2017). doi:10.1039/C7SM00356K
4. Non-Gaussian Normal Diffusion in a Fluctuating Corrugated Channel Li, F. Marchesoni, **D Debnath,** P. K. Ghosh, Physical Review Research 1, 033003(2019).
5. Diffusion of chiral janus particles in convection rolls, Y Li, L Li, F Marchesoni, **D Debnath**, PK Ghosh, Physical Review Research 2 (1), 013250 (2020).
6. Enhanced motility in a binary mixture of active nano/microswimmers, **D. Debnath**, P. K Ghosh, V. R Misko, Y. Li, F Marchesoni, F Nori, Nanoscale 12 (17), 9717-9726 (2020).
7. Escape Kinetics of an Underdamped Colloidal Particle from a Cavity through Narrow Pores, S. Nayak, T. Debnath, S. Das, **D. Debnath**, P. K Ghosh, The Journal of Physical Chemistry C, *J. Phys. Chem. C* , 124, 34, 18747–1875 (2020).

Papers presented in International/National Conference **:**

1) 'Theoretical model study on Janus particle' oral Presented in First International Online Conference on Blends, Composites, Bio-Composites and Nanocomposites (ICNC–2020), 9,10 and 11 October 2020 at Mahatma Gandhi University, Kottayam, Kerala
2) 'Active particles and diffusion' Poster Presented in International Seminar "Recent Advances in Chemistry & Material Sciences (2020)", organized by the Indian Chemical Society, 29 August, 2020.

3) 'Transport and Diffusion of self-propelled Janus Particles' Poster Presented in International Symposium on system, synthetic, & chemical biology, 5-7 December 2017, at Bose Institute, Kolkata.

4) 'Some Non Equilibrium Phenomena of Janus Particles' Poster Presented in International Symposium on Recent Advances in Chemistry and Material Sciences (2019), 2-3 August, 2019, at the Saha Institute of Nuclear Physics, Salt Lake City, Kolkata.

Signature of the Candidate

Debajyoti Debnath

(Debajyoti Debnath)

Forwarded

Pulak kr Ghosh

Dr. Pulak K. Ghosh
Assistant Professor
Department of Chemistry
Presidency University, Kolkata- 700 073

(Pulak Kumar Ghosh)
Supervisor
Assistant Professor of Chemistry,
Presidency University, Kolkata